

VARIABLE FORCE GENERATOR FOR DYNAMIC CALIBRATION OF PIEZOELECTRIC TRANSDUCERS

Juan Guerrero, Raúl Herranz

IDACOVERTRUCK, S.L.
Subdirección General de Sistemas Terrestres
INSTITUTO NACIONAL DE TÉCNICA AEROESPACIAL (INTA)
Madrid - SPAIN
jguerrero@idacovertruck.com

Abstract: Currently the calibration of dynamic load transducers is not a well resolved problem, due to the difficulty in developing a device, which gives precise dynamic force.

There are three lines of research to achieve this capacity: impact, stepped and sinusoidal forces. All of which have the same fundamentals: generation of an inertial force, which is produced by a mass and its acceleration.

At this conference, we wish to show a new line of research to produce a dynamic force based on a gyroscopic device. We have developed and tested a new device based on gyroscopic effect with the aim to calibrate piezoelectric transducers.

Keywords: calibration, piezoelectric force transducer, dynamic force, varying force and angular momentum.

1. DYNAMIC FORCE CALIBRATION. STATE OF THE ART

Normally the transducers of dynamic force are calibrated with static force or dead weight testers, taking the gravitational force into account (figure 1). The static calibration does not add knowledge about the dynamic behavior of this type of transducer [1].

It also uses calibration procedures based on the comparison with a piezoelectric sensor reference, which has been previously calibrated. In this case, the transducer is able to receive an unknown variable force (figure 1).

The calibration procedures with controlled dynamic force are not yet well developed. There is great difficulty in order to mechanically reproduce a known variable force [2]. There are three lines of research to develop variable force generators: Impact Force, Oscillation Force and Step Force [2]. The physics principle that applies to this research is Newton's 2nd law in which a force F applied to a mass m acquires an acceleration a .

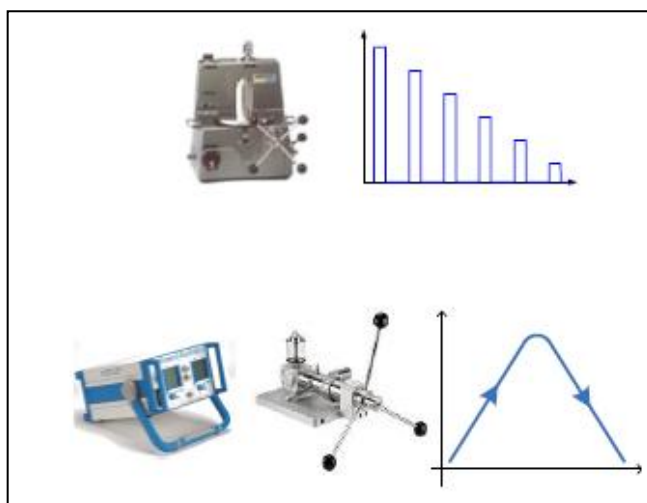


Figure 1. Stepwise calibration with a dead-weight tester (upper). Continuous comparison to a reference sensor (lower).

In the case of Impact Force (figure 2), the technology is based on a calibrated mass that deploys in a guide-way with air bearings to minimize friction. The mass impacts with the transducer for calibration. The acceleration is measured by a laser interferometer.

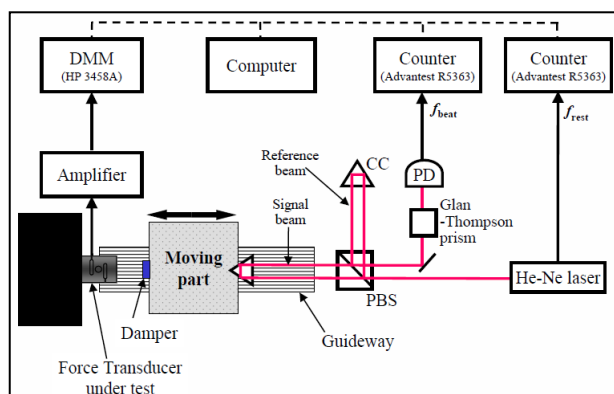


Figure 2. Setup for Impact Force Calibration (Yusaka FUJII Gunma University)

In the case of Oscillation Force (figure 3), the layout of the test is similar to the previous one, but this time, there is a spring used between the mobile mass and the transducer

where the mass is triggered by a hammer with a damper. Figure 3 is a diagram which shows this. The hammer hits the mass, and produces an oscillating movement due to the spring which is coupled between the mass and the transducer.

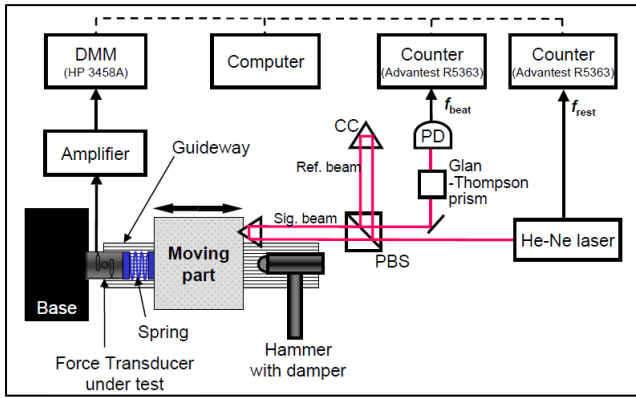


Figure 3. Setup for Oscillation Force Calibration (Yusaka FUJII Gunma University)

Finally, it can be seen in figure 4 a layout for calibration with Step Force. In this situation the mass, the guideway and the transducer are in vertical form. There is a wire which holds the mass at a specific height above the transducer. When the wire is released, the mass accelerates by the action of gravity and hits the transducer and produces a stepped reaction.

There are other methods to calibrate this type of transducers, as described in [3] based on the Hopkinson Bar for Impact Force, or through shakers [1], [4] for oscillation forces.

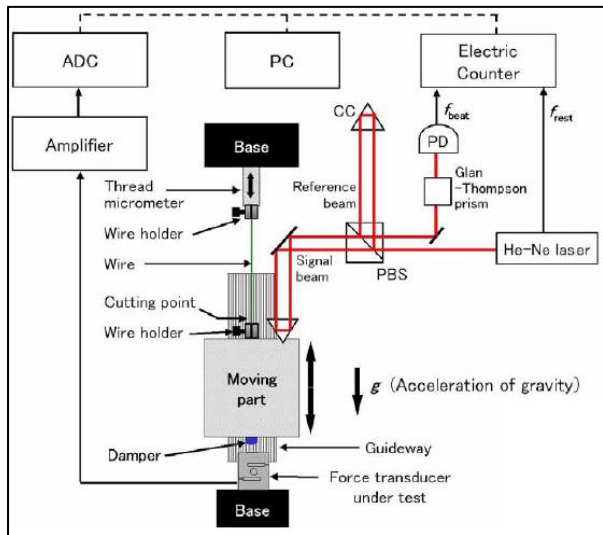


Figure 4. Setup for Step Force Calibration (Yusaka FUJII Gunma University).

2. A NEW PHYSICAL CONCEPT FOR ACHIEVING VARIABLE FORCE

In order to produce a variable force with previously known values, we base this on a different principle which

uses the lines of investigation previously mentioned (Newton's 2nd law). Our line of investigation is based fundamentally on the conservation of angular momentum, which establishes the angular momentum of a system, which remains constant unless acted on by an external torque.

The following is going to explain how this law is applied to our mechanism.

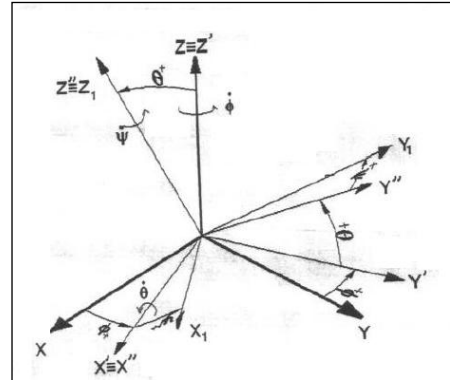


Figure 5. Euler Angles which describe the orientation of a rigid body with respect to a fixed coordinate system.

Figure 5 exposes how any angular orientation of a rigid body can be described by a sequence of three angular transformations. These three angles are called Euler angles:

- ϕ Precession. Rotation around Z
- θ Nutation. Rotation around X'
- ψ Nutation. Rotation around Z''

If the hypothetic body is turning with a specific velocity of gyro ω , its components (p, q, r) in a non-inertial reference system are as follow [5]:

$$\omega = \begin{bmatrix} p \\ q \\ r \end{bmatrix} = \begin{bmatrix} \dot{\phi} \sin\theta \sin\psi - \dot{\theta} \cos\psi \\ \dot{\phi} \sin\theta \cos\psi - \dot{\theta} \sin\psi \\ \dot{\psi} + \dot{\phi} \cos\theta \end{bmatrix} \quad (1)$$

The angular momentum is defined as $\mathbf{H} = \mathbf{I}\omega$, and the conservation law establishes: $\frac{d}{dt} \mathbf{H} = \mathbf{N}$

Where \mathbf{H} is the angular momentum, \mathbf{I} is the inertia tensor and \mathbf{N} is the momentum of external loads with respect to centre of masses.

When a momentum \mathbf{N} with components N_1, N_2, N_3 is applied to a rigid body, the system of equations which corresponds to its turning is [6]:

$$\begin{aligned} I_1 \dot{p} - (I_2 - I_3)qr &= N_1 \\ I_2 \dot{q} - (I_3 - I_1)rp &= N_2 \\ I_3 \dot{r} - (I_1 - I_2)pq &= N_3 \end{aligned} \quad (2)$$

This system of equations establishes the relationship between the load applied to a rigid body (N_1, N_2, N_3) and its kinematic response, given by the components of the vector ω , and its angular accelerations ($\dot{p}, \dot{q}, \dot{r}$).

In exchange, if the rigid body is loaded with an angular velocity ω , instead of a momentum N , and the body is restricted in gyros, then the momentum reactions ($N_x, N_y,$

N_z) appear on the restrictions. The next equation gives the relationship:

$$\begin{bmatrix} N_x \\ N_y \\ N_z \end{bmatrix} = R^T \cdot \begin{bmatrix} N_1 \\ N_2 \\ N_3 \end{bmatrix} \quad (3)$$

R^T is the transposed transformation array. R is as follows:

$$R = \begin{bmatrix} \cos\psi\cos\phi - \cos\theta\sin\psi\sin\phi & \cos\psi\sin\phi + \cos\theta\sin\psi\cos\phi & \sin\theta\sin\psi \\ -\sin\psi\cos\phi - \cos\theta\cos\psi\sin\phi & -\sin\psi\sin\phi + \cos\theta\cos\psi\cos\phi & \sin\theta\cos\psi \\ \sin\theta\sin\phi & -\sin\theta\cos\phi & \cos\theta \end{bmatrix} \quad (4)$$

The mechanism presented in this lecture follows the previous theory. It is formed by two rotating disc (a, b) that are spinning and turning on a nutation angle with the same moment of inertia ($I_{1a} = I_{1b}, I_{2a} = I_{2b}, I_{3a} = I_{3b}$), and the vectors of both gyros are disposed in parallel planes. The moment of inertia in the Y axis for both discs is $I_{3a} = I_{3b}$.

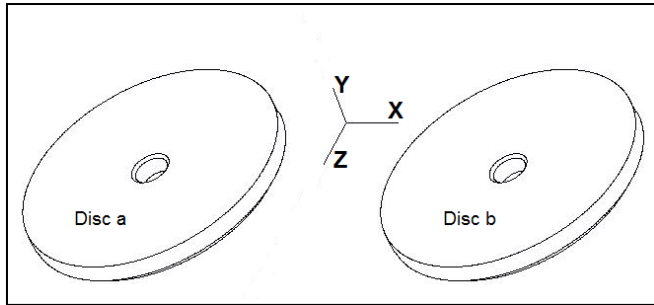


Figure 6. Rotating discs referenced to the inertial coordinate system.

Taking into account these arrangements, it happens that the precession value is null ($\phi = 0$). Moreover, the moments of inertia take the following values:

$$\begin{aligned} I_1 &= I_2 = I \\ I_{3a} &= I_{3b} = I_3 \end{aligned} \quad (5)$$

Thus, processing with previous equations:

$$\omega = \begin{bmatrix} p \\ q \\ r \end{bmatrix} = \begin{bmatrix} \dot{\theta} \cos\psi \\ -\dot{\theta} \sin\psi \\ \dot{\psi} \end{bmatrix} \quad (6)$$

$$\dot{\omega} = \begin{bmatrix} \dot{p} \\ \dot{q} \\ \dot{r} \end{bmatrix} = \begin{bmatrix} \ddot{\theta} \cos\psi - \dot{\theta} \dot{\psi} \sin\psi \\ -\ddot{\theta} \sin\psi - \dot{\theta} \dot{\psi} \cos\psi \\ \ddot{\psi} \end{bmatrix} \quad (7)$$

$$R = \begin{bmatrix} \cos\psi & \cos\psi\sin\phi & \sin\theta\sin\psi \\ -\sin\psi & \cos\theta\cos\psi & \sin\theta\cos\psi \\ 0 & -\sin\theta & \cos\theta \end{bmatrix} \quad (8)$$

Momentum given by each disc is this:

$$-N_x = I\ddot{\theta}$$

$$\begin{aligned} -N_y &= -I_3\ddot{\psi}\sin\theta - I_3\dot{\psi}\dot{\theta}\cos\theta \\ -N_z &= -I_3\ddot{\psi}\cos\theta - I_3\dot{\psi}\dot{\theta}\sin\theta \end{aligned} \quad (9)$$

As the rotating form of each disc, follows this assumption:

$$\theta_a = -\theta_b$$

Then (9), by the addition of each disc, yields:

$$\begin{aligned} -N_x &= 0 \\ -N_y &= -2I_3\ddot{\psi}\sin\theta - 2I_3\dot{\psi}\dot{\theta}\cos\theta \\ -N_z &= 0 \end{aligned} \quad (10)$$

Finally, it is considered constant spinning: $\dot{\psi}_a = -\dot{\psi}_b = 0$,

$$N_y = 2I_3\dot{\psi}\dot{\theta}\cos\theta \quad (11)$$

In conclusion, only the component Y of momentum appears, which is sinusoidal with the amplitude given by the factor $2I_3\dot{\psi}\dot{\theta}$ and it has a frequency given by the nutation velocity $\dot{\theta}$, therefore it is correct to rewrite the equation as follows:

$$N_y(\theta) = 2I_3\dot{\psi}\dot{\theta}\cos\theta \quad (12)$$

The machine transforms this momentum in a variable force, by means of a shaft that receives this momentum and alternatively pulls a rod. The rod comprises a piezoelectric force transducer, in order to obtain its calibration with the variable force produced.

Equation (12) is very important as it has been obtained without any approximation, i.e. the equation is exact. Therefore, it has become the Standard of the 1st level in order to calibrate any similar machine based on the conservation of the law of angular momentum, for variable force and momentum magnitudes.

3. DESCRIPTION OF THE VARIABLE FORCE GENERATOR

The mechanism is designed to actuate over two discs (figure 6) and signifies both spinning and nutation angles.

These turn velocities are achieved by three motors: two for the spinning of each disc and the third for rotating in nutation both discs. Figure 7 shows the arrangement. The nutation motor by means of the bevel gear box, achieve turn the discs and their respective motors in opposite senses while both disc are spinning.

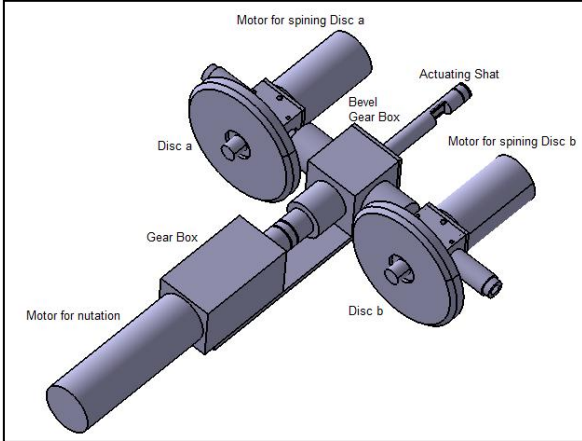


Figure 6. Basic elements for moving discs *a*, *b* in order to produce spinning and nutation gyros.

Consequently of combined gyros, the actuating shaft exerts the momentum according to equation (12). This moment is transformed in a variable force for pulling the piezoelectric force transducer (figure 7).

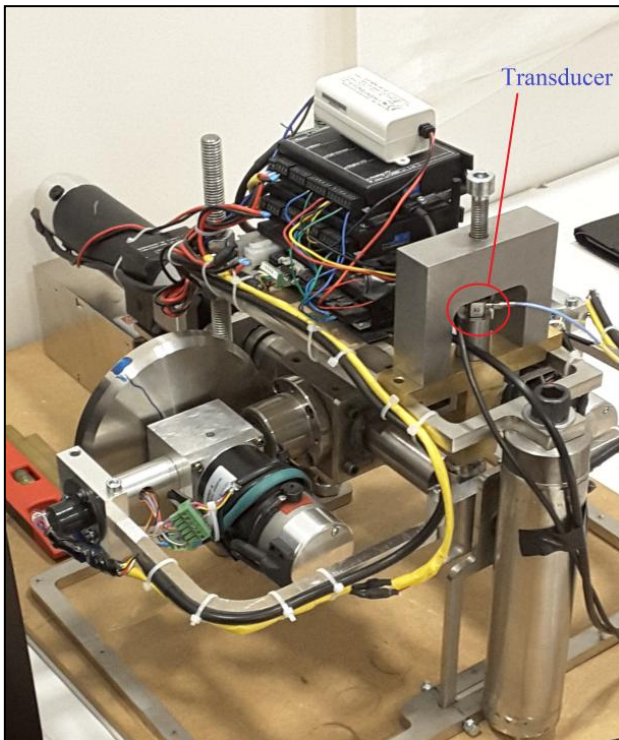


Figure 7. Variable Force Generator. The Transducer to be tested is indicated.

In summary, the mechanism generates a previously known variable force, which is applied to the transducer. This consequently results in the transducer generating a proportional signal to the supported variable force. The

force achieved by the mechanism and the generated signal by the transducer are compared, making it possible for the transducer to be calibrated.

The basic magnitudes involved are time, angle and moment of inertia. The last one remains constant. There are no hysteresis cycles during operation. On the other hand, no physical properties of components are involved, such as rigid (spring) or damping constants. This is why the reproducibility of the test is very good.

Currently the mechanism is in prototype stage, and is being tested with piezoelectric transducers with the purpose of evaluating their real capacities.

4. TESTING THE VARIABLE FORCE GENERATOR

As previously indicated, the mechanism could be characterized according to equation (12). This equation establishes the perfect generation for the variable moment, and the variable force is generated as follows:

$$F(\theta) = N_y(\theta) \cdot l \quad (13)$$

Where *l* is the length of the arm that converts the momentum to force.

Consequently, the correct behavior of the mechanism depends on the following variables:

Spin <i>a</i> and <i>b</i>	ψ_a, ψ_b
Nutation	θ
Inertia <i>a</i> and <i>b</i>	I_a, I_b
Arm	l

The product $\psi\dot{\theta}$ belonging to equation (12) has been tested. The procedure followed record the spin values of each disc's motors and determined the error according to the expression:

$$error = \left| \frac{\dot{\theta}_r \psi_r - \dot{\theta}_t \psi_t}{\dot{\theta}_t \psi_t} \right|_{\theta}$$

Where the subscript *r* references the data recorded of the motors' encoder and *t* references the value from equation (12).

Results are plotted in figure 8. Where four cases are presented:

Table 1. Cases tested to assess the product of turning velocities.

Case	Spin (rpm)	Nut. Velocity (rpm)
1	1800	600
2	1800	1200
3	1800	1500
4	2340	1154

The graph shows most of the values in a range of $\pm 2\%$.

Next, the magnitude to be considered is the momentum of inertia. Although the momentum of the inertia of the discs is known ($0.00475 \text{ kg}\cdot\text{m}^2$) due to their geometry and material density (steel $7850 \text{ kg}/\text{m}^3$), the total rotary momentum of inertia is not known (shafts, nuts, washers and rotary parts of motors). In order to obtain these values for each disc, a series of tests have been developed. These tests were performed with the acceleration of each disc by its respective motor with a constant torque. The momentum of inertia can be obtained through the following expression:

$$I = \frac{N}{\alpha}$$

With I as the moment of inertia, N torque and α turning acceleration.

The next table summarizes the results.

Table 2. Inertias for rotating sets.

	Left Motor	Right Motor
Inertia ($\text{kg}\cdot\text{m}^2$)	0.006101	0.006271

Finally, in order to test the mechanism a piezoelectric transducer of 5kN has been used from the company HBM

(CFT/5kN) and a charge amplifier (CMD600) also from HBM.

Here, we present a trial aimed at obtaining the repetition capacity of the machine, acting on the indicated piezoelectric transducer.

For this, two series of trials have been done.

Series 1. Three tests were done, each one with a sinusoidal signal of 10 pulses with a maximum value of 860 N and at the frequencies: 0.56, 1.11 and 1.67 Hz. See figure 9.

Series 2. Three tests were done, each one with a sinusoidal signal of 10 pulses with a maximum value of 1700 N and at the frequencies: 0.91, 1.07 and 1.28 Hz. See figure 10.

In each test (see Table 3 and Table 4), the maximum values obtained by the transducer are recorded for each cycle and the mean and the standard deviation and their ratios are calculated with respect to the average value. In the two tables, these values are presented, as well as the speed of the gyro spin and nutation for each test.

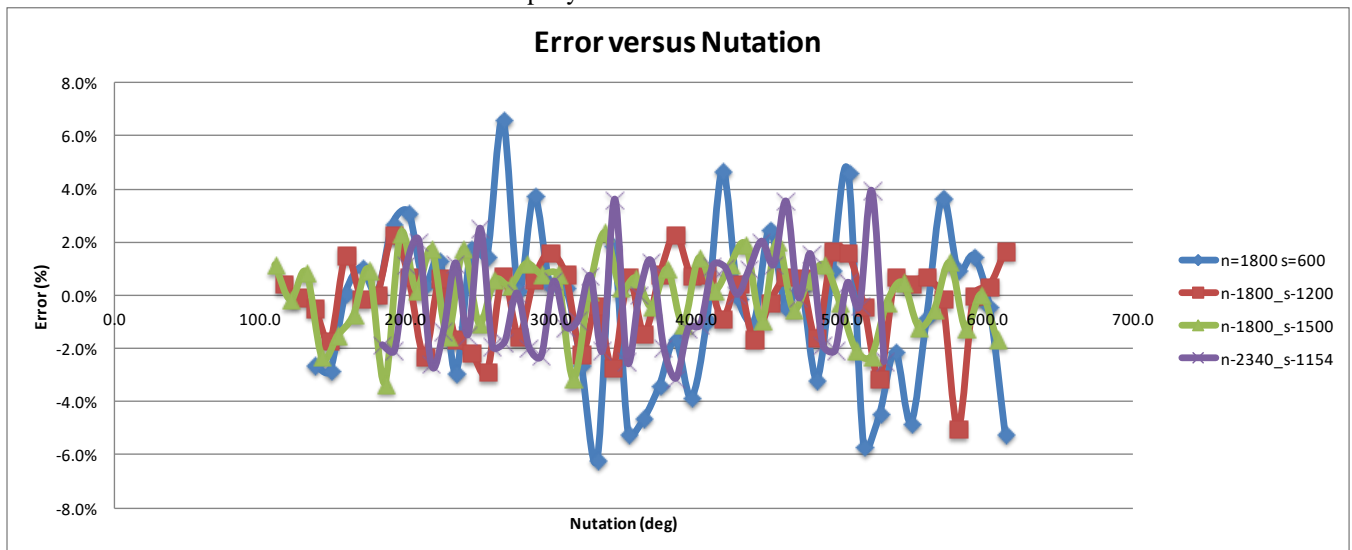


Figure 8. Errors produced measuring spin and nutation velocity take account four cases.

Table 3. Results obtained for Series 1

	Nutation θ (Hz)	Spin ψ' (Hz)	$\theta \cdot \psi'$ (Hz^2)	Maximum Values (N)										Mean	Std Dev	%
				1	2	3	4	5	6	7	8	9	10			
Test 1	0.56	47.93	26.84	858	843	848	869	870	863	842	826	857	872	855	14.9	1.75%
Test 2	1.11	24.03	26.67	-	869	880	860	873	877	876	890	889	894	879	11.1	1.26%
Test 3	1.67	15.99	26.70	-	-	876	878	868	869	866	867	872	-	871	4.5	0.51%

Mean 868.03 N
 Std Dev 12.26 N
 % 1.41%

Table 4. Results obtained for Series 2

	Nutation θ (Hz)	Spin ψ' (Hz)	$\theta \cdot \psi'$ (Hz ²)	Maximum Values (N)										Mean (N)	Std Dsv (N)	%	
				1	2	3	4	5	6	7	8	9	10				
Test 1	0.92	58.4	53.73	1666	1664	1670	1652	1661	1666	1675	1671	1651	1667	1664	7.7	0.46%	
Test 2	1.07	50	53.50	1663	1595	1669	1666	1707	1667	1639	1637	1719	1665	1663	34.9	2.10%	
Test 3	1.28	41.7	53.38	1803	1786	1807	1750	1776	1798	1792	1761	1736	1725	1773	29.1	1.64%	
				Mean		1685.50 N											
				Std Dev		33.89 N											
				%		2.01%											

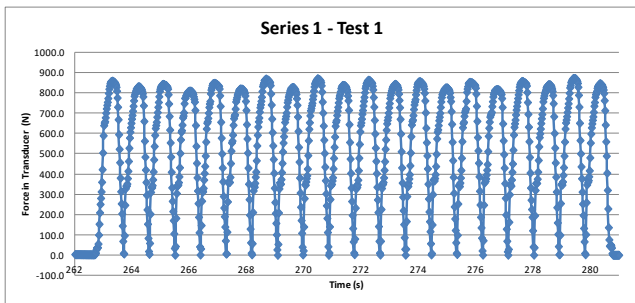


Figure 9. Variable Force read by the Transducer. Only odd pulses are taken into account.

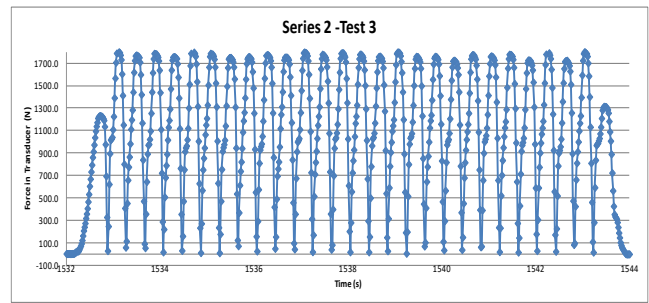


Figure 10. Variable Force read by the Transducer. Only even pulses are taken into account and extreme pulses are excluded.

5. CONCLUSIONS

We present the capabilities of a mechanism designed to make dynamic calibrations of piezoelectric force transducers, which is being newly based on the conservation of angular momentum.

The mechanism generates sinusoidal signals of force in which there can be several cycle frequencies for a same maximum value or maximum values at the same frequency. These variations are achieved by acting on the discs, with two types of gyros (spin and nutation) and a same moment of inertia.

The capabilities of the mechanism are being analyzed and a high degree of repetition has been verified in the tests that have been done, despite being in its prototype phase.

The prototype has been referenced in equation (12) which represents the 1st Standard for this new type of measuring machine.

6. REFERENCES

[1] R. Kumme, G. Lauer, M. Peters, A. Sawia, "Development of Methods for Dynamic Force Calibration Part 1, Dynamic Calibration of Force Transducers based on the Determination of Inertia Forces with Interferometric Calibrated Acceleration Transducers", Preface, APPLIED METROLOGY, COMMISSION OF THE EUROPEAN COMMUNITIES, Report EUR 12933/1 EN, 1990.

[2] Yusaku Fujii, "Dynamica Calibration Methods for Force Transducers", XVII IMEKO WORLD CONGRESS, Metrology for a Sustainable Development, September, 17 – 22, 2006, Río de Janeiro, Brazil.

[3] Diederik Van Nuffel, et all., "Calibration of Dynamic Piezoelectric Force Transducers Using the Hopkinson Bar Technique", 15th International Conference on Experimental Mechnics, Paper Ref: 3068.

[4] Christian Schlegel, et all., "Dynamic Calibration of Force Transducers Using Sinusoidal Excitations", The Second International Conference on Sensor Device Technologies and Applications, SENSORDEVICES 2011.

[5] Jesús Gómez Pardo, "Actuador Giroscópico Avanzado para Control de Satélites Ágiles", Tesis Doctoral, Escuela Politécnica Superior del Ejército, Spain, 2010.

[6] Goldstein H. "Mecánica Clásica", Colección Ciencia y Tecnología. Editorial Aguilar. Segunda Edición 1977.